



Phytoplankton, Bacteria and Heterotrophic Nanoflagellate studies using ship and OCM-2 data along a coastal transect in the Arabian Sea

S. G. Prabhu Matondkar¹, S. Basu¹, Sushma G. Parab¹, Suraksha Pednekar¹, Niyati Hede¹, R. M. Dwivedi², Mini Raman², K. N. Babu², A. K. Shukla² and M. M. Shirdhankar³

¹National Institute of Oceanography, Dona Paula, Goa

²Space Application Centre, Ahmedabad

³Ratnagiri College of Fisheries, Ratnagiri

Abstract

The coastal region of the Central West coast of India is biologically productive and is well known for its Mackerel and Sardine fishery. December is an active fishing month and it just happens to fall in the post-monsoon period when coastal waters are influenced by the riverine discharge of fresh-water. The impacts of fresh-water on the components of the food chain were studied on a cruise conducted on-board the coastal research vessel *Sindhu Sankalp*. A total of 40 stations distributed over 3 transects were sampled like those found off the coast of Goa, off Ratnagiri and off Dabhol. Physical conditions like salinity and temperature were monitored. Salinity of coastal waters ranged from 33.93 - 34.59 psu which lowered sigma-t values from 24.08 - 21.49 kg m⁻³ to 22.57 - 21.92 kg m⁻³ due to fresh-water run-off during the extended monsoon of 2010. Chlorophyll a (Chl a) values of the coastal waters were 2.98 ± 0.83 µg L⁻¹ (estimated) and 2.85 ± 0.73 µg L⁻¹ (OCM-II), which was much higher than shelf stations ranging 1.57 ± 1.15 µg L⁻¹ (estimated) and 0.92 ± 0.42 µg L⁻¹ (OCM-II). Further, we have estimated other components of this productive ecosystem including the total bacterial loads and Heterotrophic Nanoflagellate (HNF) population. The total bacteria of coastal waters ranged from 0.93x10⁹ - 4.359x10⁹ cells L⁻¹. A strong positive correlation was noticed in Chl a and bacterial load, especially in shelf waters (R² = 0.839, n=13, p<0.0001). Further, HNF as grazer showed a negative pattern with the bacteria and hence the phytoplankton biomass. The HNF population was found to be high in shelf waters (2.97±1.16 x10⁶ cells L⁻¹) when compared to that found in

turbid coastal waters ($1.53 \pm 0.47 \times 10^6$ cells L^{-1}). Further, the bacterial load showed an appreciably higher relationship with CDOM in the shelf waters off the west coast of Ratnagiri ($R^2=0.85$, $n=8$, $p<0.0001$) when compared to that found in coastal waters ($R^2=0.245$, $n=24$, $p<0.001$). CDOM Ac325 in coastal water ranged from $0.51 - 1.32 \text{ m}^{-1}$ which is reasonably high compared to the CDOM values in the shelf waters of $0.228 - 1.209 \text{ m}^{-1}$. The use of OCM-II data for understanding the impact of the monsoon on the food-chain was explored and has been presented in order to understand the pattern, in both the bacterial and the HNF biomass based on the chlorophyll values retrieved from OCM images.

Key Words:

Phytoplankton, Bacteria, HNF, C-DOM, Sardines, OCM-II

Introduction

Marine environments are classified as Case-I and Case-II waters based upon optical properties of the waters (Morel and Prieur, 1977). Case-I waters contain phytoplankton (and bacteria), detrital matter and colored dissolved organic matter (C-DOM) which are well correlated with Chlorophyll *a* (Chl *a*) concentrations. Chl *a* (phytoplankton) chiefly contribute to inherent and apparent optical properties of the water-mass. We are attempting here to express ecosystem component as the function of Chl *a* concentration. Turbid and optically complex coastal waters fall under case-II category, where C-DOM and suspended sediment interfere with optical properties.

There is a lack of measurement in the Case-II waters along West-coast of India, where monsoon and river-run-off dominates. This data can be used for fishery prediction, fishery management and understanding climate change in the Arabian Sea. The use of OCM derived Chl *a* requires these data sets for applying Case-I algorithms for Case-III waters if possible, and now to improve it. We are trying to see accuracy of OCM-II derived Chl *a* in case-II waters and its application for understanding food-chain dynamics in this region.

South-West monsoon brings upwelled water with high nutrients in the coastal waters of the Arabian Sea. River run-off by several rivers in the Arabian Sea also transports nutrients. The

productive region support rich fishery, specially sardines, mackerels (pelagic) and prawns (demersal). The growth of phytoplankton fuelled by nutrients gives rise to swarms of zooplanktons and shoals of the fishes. We are trying to understand ecosystem components during this period and use of remote-sensing for the same. Chl *a* and temperature data from sensors are routinely used to predict Fishery Potential Zones (FPZ), mostly in case-I waters (Solanki et al., 2005). This exercise is mainly for case-II waters, since majority fishery resources are in Case-II waters.

Materials and Methods

Sampling

During cruise CRV *Sindhu Sankalp* 009 (SSK-009), water samples were collected from three transects off Goa, Ratnagiri and Dabhol-Shivardhan in the Eastern Arabian Sea (Fig. 1). 10 L Niskin sampling bottles used for sampling were mounted onto a Sea Bird Electronics® CTD rosette. Stations off Goa and Ratnagiri transects were perpendicular to the coast and comprised of coastal, shelf and slope waters while stations off Dabhol-Shivardhan transect were parallel to the coast representing near-shore waters of ~10-15m depths.

Hydrological data

At each station, the Sea Bird CTD profiler was used to obtain vertical profiles of temperature, salinity and density (sigma-t) and data processing was done via Seasave V7.

OCM-II image Analysis

OCM-II level 2c images of the during December 2010 in the Arabian Sea were also obtained as .hdf files from National Remote Sensing Centre (NRSC), Hyderabad, India and were further processed using ERDAS 9.5 or ENVI 4.4 at Space Application Centre (ISRO), Ahmedabad to retrieve Chl*a*.

Chlorophyll a

Phytoplankton biomass estimated as Chlorophyll *a* was determined by 90% acetone extraction method. Chl *a* was estimated using HPLC (Agilent® 1100 series) where pigment

separation was done in C-18 reverse phase column using the eluent gradient program (Parab et al., 2006) using DHI, Denmark pigment standards.

Bacterial abundance

For enumeration of bacteria, water samples were fixed with 2% final concentration (v/v) of glutaraldehyde and stored at 4°C during the cruise. Aliquots of 5-15mL water samples were stained with DAPI (Porter et al., 1980) and filtered through black polycarbonate filters (0.22 µm pore size, Nuclepore). Filters were mounted on glass slides and at least 600 cells from 10-25 fields were counted under an eyepiece with 100×100 µm counting grid and ×100 objectives using a Nikon 80i epifluorescence microscope (Hobbie et al., 1977) fitted with UV filter sets.

Heterotrophic Nanoflagellates (HNF)

Samples for Nanoflagellates enumeration were size fractionated through 20µm nylon mesh. 100 ml of sea water was fixed in a three step procedure: 0.05% final concentration of alkaline Lugol's solution, followed by addition of 0.1% final concentration of 3% sodium thiosulfate and 2% final concentration of borate buffered formalin (Sherr and Sherr, 1993). 25-50 ml of preserved sub-samples were used for slide preparation. The first set was stained with 50 µg ml⁻¹ DAPI (4',6'-diamidino-2-phenylindole) for 7-10 mins and filtered through 0.8 µm pore-size Nuclepore polycarbonate filters. Filters were mounted on glass slides and at least 200 cells from 40 fields were counted under an eyepiece with 100×100 µm counting grid and ×100 objectives using a Nikon 80i epifluorescence microscope with UV filter sets. Distinction for autotrophic flagellates was made on the basis on their autofluorescence under Blue filter set.

Chromophoric Dissolved Organic Matter (C-DOM)

Clean techniques were employed to obtain the dissolved fraction of sea-water samples after filtration through 0.22 micron Nuclepore filter using a low pump pressure (~5mmHg). Absorbance characteristics of the dissolved fraction (CDOM) were measured by UV/Vis spectrophotometer (Model. Perkin Elmer lambda 40) on-board using a quartz cuvette of 10 cm

path-length. Analyses for all CDOM samples were immediately carried out within half an hour of sample collection during the entire cruise.

Characteristic absorption spectra were obtained for the 200–800 nm regions and absorption coefficients were calculated after scattering/baseline corrections (Basu et al. 2011) as:

$$Ac_{\lambda} = 2.303A/l$$

where, Ac_{λ} is the absorption coefficient (m^{-1}) corresponding to absorbance A at wavelength λ and l is the optical path length (m). CDOM concentration was measured as absorption coefficient at 325 nm (Ac_{325}) (Nelson and Siegel 2002) and chemical nature of CDOM were studied in terms of the Slope-ratio ($S_{Ratio} = S_{275-295} : S_{350-400}$) to effectively distinguish near-shore/coastal shelf and slope water characteristics as previously described (Helms et al. 2008).

Statistical analysis

Correlation and linear regression analysis for evaluating relationship of trophic components were performed using MS Excel and Origin 6, while Contour figures were plotted via Ocean Data View 4 software. Comparative depth profiles of microbial web components were drawn using Grapher 8 (Golden Software, Inc).

Results and Discussion

Water-column characteristics

Being typical post-monsoon season (December 2010), low salinity was observed at surface as well as sub-surface layers. Salinity was in the range of 33.9 - 34.5 psu (Fig. 2). Since water-column was well mixed at most of the stations, low salinity is also observed at sub-surface layers. The low saline water reached upto 80m depth zone where oxygen was as low as 18-25 μ M (Fig. 2).

Temperature of near-shore region was low $\sim 26^{\circ}$ C compared to deeper zone which was $\sim 27^{\circ}$ C. The low temperature was mainly due to fresh-water from river discharge. The temperature inversion was recorded in Ratnagiri shelf region due to fresh-water cap and sea-water underlying that low saline water.

Nutrient analysis indicated low nitrate at majority of the stations. The nitrate added by coastal upwelling and river discharge gets utilized during October-November months. Low nitrate concentration particularly reflected in the low phytoplankton biomass in the study area.

Chlorophyll a distribution

In general, Chl *a* is low since water is turbid as well as low in nitrate and oxygen content. Off Goa and Ratnagiri, Chl *a* was in the same range as $\sim 0.6 \mu\text{g L}^{-1}$. However, off Dabhol high Chl *a* in the range of $1.83 \pm 0.69 \mu\text{g L}^{-1}$ was recorded (Fig. 6). The region supports appreciable Sardine fishery, maintaining Chl *a* at low concentrations during the study-period due to intense grazing.

Chromophoric dissolved organic matter characterization

Chromophoric dissolved organic matter is high due to the influence of the river discharge. The C-DOM absorption values A_{c325} are similar at Goa (~ 0.58) and Ratnagiri transect (~ 0.6) but reasonably high in the off Dabhol area (~ 0.74). In the turbid coastal water Chl *a* and C-DOM relationship is poor whereas, in the slope and shelf waters C-DOM showed improved relationship with Chl *a* ($R^2 = 0.2 - 0.35$) and is of phytoplankton origin (Fig. 10).

Microbial Trophic components

Total bacterial counts are proportional to Chl *a* (Fig. 8). High counts are recorded in turbid Dabhol waters ($2.29 \pm 0.843 \times 10^9 \text{ cells L}^{-1}$) compared to Goa ($\sim 0.87 \times 10^9 \text{ cells L}^{-1}$) and Ratnagiri waters ($\sim 1.54 \times 10^9 \text{ cells L}^{-1}$). Naturally bacterial relationship with CDOM is also poor (Fig. 9).

Heterotrophic Nanoflagellate (HNF) counts were low in the turbid waters off Dabhol, whereas bacterial counts and CDOM values were high. However, HNF population was high in Goa waters where C-DOM concentration and bacterial counts are low (Fig. 6 and 7).

The overall inverse relationship obtained between bacteria and HNF is presented in Fig. 8. HNF counts are $3.63 \pm 1.13 \times 10^6 \text{ cells L}^{-1}$ in Goa water and $1.53 \times 10^6 \text{ cells L}^{-1}$ in the Dabhol water (Fig. 8). These relationships are also reflected in the nature of the vertical profile of the Chl *a*, bacterial counts and the HNF counts (Fig. 7). However, Chl *a* to primary-production relation is reasonably good ($R^2 = 0.465$, $n=63$) as depicted in Fig. 11b. Thus, the component of

ecosystem like Chl *a* (Phytoplankton), Heterotrophic Nanoflagellates (grazers), bacterial (mineralizers) and C-DOM as the food for heterotrophs as well as rate of primary-production are coupled and hence predictable based upon *insitu* Chl *a* and Chl *a* retrieved by the OCM-II and other sensors.

Of particular relevance to energy and material cycling in the marine habitat is the trophic relationship between algae and heterotrophic bacteria (Stewart et al. 2004). This relationship develops primarily when bacteria assimilate dissolved organic matter (DOM) generated from phytoplankton via processes extracellular exudation like rupture and degradation of phytoplankton cells during grazing, viral lysis and/or direct extracellular release (Larsson and Hagstrom 1979; Wolter 1982; Moller 1993). Bacterial assimilation of DOM is a core process in the “microbial loop” that cycles dissolved products of photosynthesis back to plankton food web during grazing by nanoflagellates (Azam et al. 1983; Strom 2000).

Our data shows high abundance of total bacterial counts in the Eastern Arabian Sea water-column in the range of $\sim 1 \times 10^9$ cells L⁻¹ similar to previous reports (Ramaiah et al. 1996). Regression analysis shows that bacteria and Chl *a* are strongly correlated off Ratnagiri transect ($R^2=0.839$, $n=13$) and not C-DOM (Fig. 8). This possibly indicates strong bacterial preference for labile phytoplankton exudates rather than DOM from terrigenous run-offs. Bacteria and algae had no discernible relationship in the water column off Goa. A hypothesis compatible with our data is that bacterial populations off Goa transect may be suppressed by HNF grazing. In contrast, HNF grazing control may be weaker off Ratnagiri and Dhabol-Shrivardhan transect, allowing bacteria to increase more steeply with algal biomass. Significant positive relationship between pelagic bacterial abundance and Chlorophyll *a* (Chl *a*) concentration have been reported from both case-I and Case-II waters (Linley et al. 1983; Lochte et al. 1997). Conversely, instances when bacterial biomass or production doesn't increase with increasing chlorophyll *a* and primary production has also been noted (Bird and Karl 1999).

Biological top-down control of microbial biomass involves grazing of bacteria and algae by protists and microzooplankton (Stewart et al. 2004). The overall inverse relationship as seen in the present study between bacteria and HNF has also been reported across a wide diverse systems as $R^2 < 0.25 < 0.01$ (Gasol and Vague 1993). However, a strong positive relationship between bacteria and HNF has also been noted (Krstulovic et al. 1997). Overall, HNF abundance gradually decreased on moving North from Goa to Dhabol-Shrivardhan transect. This may be

due to grazing by microzooplanktons that quickly responded to an increase in HNF (Gasol and Vague 1993).

The major characteristics of C-DOM in the study area are observed to be of low slope-ratio indicating humic nature and also terrestrial origin from run-offs (Fig. 10). Off Goa transect C-DOM with very low-slope ratios (similar to terrestrial C-DOM) occurred in the bottom waters of both shelf and the slope. This raises questions on their possible diagenesis and is explained due to advection and sinking of run-off originated C-DOM during the monsoon into the deeper waters. Although Chl *a* is strongly related to bacterial counts ($R^2 = 0.648$, $n=63$), relationship between CDOM remains insignificant ($R^2 < 0.1$, $n=63$). Insignificant relationship with bacteria and CDOM and also between CDOM and Chl *a* is further reflected in the coastal and shelf waters as well as deeper waters off Goa, Ratnagiri and in the near-shore waters off Dabhol-Shivardhan. The strong relation between Chl *a* and bacteria across all the transects seems to suggest that phytoplankton derived organic matter may be most preferential source of nutrition for bacteria. The dissolved organic carbon (DOC) derived from phytoplankton is highly amenable to bacterial growth which include carbohydrates, followed by nitrogen compounds, namely proteins, polypeptides and amino acids (Cole et al. 1988). However, strong positive relationship of bacterial abundance with chl *a* ($R^2=0.65$, $p<0.01$) and CDOM concentration ($R^2=0.8373$, $p=0.01$) during blooms of *Trichodesmium* spp. has also been reported in the Eastern Arabian Sea (Basu et al. 2011).

In view of this, it appears that CDOM during post-monsoon period is of a mixed character – that of high and low slope ratios, detected in coastal/shelf as well as deeper slope waters and hence the insignificant relationships. Following an extended monsoon, the nature of this CDOM is less suitable for quick bacterial utilization. Loading of allochthonous DOC would not necessarily stimulate bacteria production and hence carbon transfers via food web. Our results show strong relationship with Chl *a* and bacteria suggesting that bacterial abundance is controlled by phytoplankton based DOM via grazing food-chain, rather than high concentrations of low-slope ratio terrestrial CDOM following monsoon. The origin of high concentrations of low slope-ratio CDOM off Goa, which is may be of higher molecular weight is however not clear and their microbial recycling in anoxic waters may be biogeochemically significant.

An excellent relationship is being established between OCM-II derived Chl *a* and insitu measurements from present study (Fig. 4). As it is observed earlier, Chl *a* is positively/negatively

related to bacteria, HNF and CDOM, where Chl *a* data can be used to predict above components. Recently, remotely derived Chl *a* was also found to be useful to predict Sardine fishery (George et al., 2012). The region under study is an important site along West-coast for Sardine fishery. The variations in the fishery can be well understood by monitoring components like Chl *a*, C-DOM, flagellates etc. The data can be also useful to map areas for primary-productivity measurements. This will be important contribution towards optical biogeochemistry of the Arabian Sea.

Acknowledgements

Thanks are due to Director National Institute of Oceanography, Goa and Director, Space Application Centre (SAC) for encouragement and support. We are thankful to Shri Sanket Ponshe and Shri Abhijit Thakre from Fishery college of Ratnagiri for help during Sindhu Sankalp cruise.

References

1. Azam F, Fenchel T, Field JG, Gray JS, Meyer-Riel LA, Thingstad F (1983) The ecological role of water-column microbes in the sea. *Mar Ecol Prog Ser* 10:257–263.
2. Basu S, Matondkar SGP, Furtado I (2011) Enumeration of bacteria from a *Trichodesmium* spp. Bloom of the Eastern Arabian Sea: elucidation of their possible role in biogeochemistry. *J Appl Phycol* 23 (4):309-319.
3. Bird DF, Karl DM (1999) Uncoupling of bacteria and phytoplankton during the austral spring bloom in Gerlache Strait, Antarctic Peninsula. *Aquat Microb Ecol* 19: 13-27.
4. Cole JJ, Findlay S, Pace ML (1988) Bacterial production in fresh and salt water system: a cross-system overview. *Mar Ecol Prog Ser* 43:1–10.
5. Gasol JM and Vaque D (1993) Lack of coupling between heterotrophic nanoflagellates and bacteria: a general phenomenon across aquatic systems? *Limnol Oceanogr* 38:657-665.
6. George G, Meenakumari B, Raman M, Kumar S, Vethamony P, Babu MT, Verlecar X (2012) Remotely sensed Chlorophyll: A putative trophic link for explaining variability in Indian oil Sardine stocks. *J Coastal Res* 28(1A):105-113.

7. Helms RJ, Stubbins A, Ritchie DJ, Minor CE, Kieber JD, Mopper K (2008) Absorbance spectral slopes and slope ratios as indicators of molecular weight, source and photobleaching of Chromophoric dissolved organic matter. *Limnol Oceanogr* 53:955–969.
8. Hobbie JE, Daley RJ, Japer S (1977) Use of Nuclepore filters for counting bacteria by fluorescence microscopy. *Appl Environ Microbiol* 33:1225–1228.
9. Krstulovic N, Solic M, Marasovic I (1997) Relationship between bacteria, phytoplankton and heterotrophic nanoflagellates along the trophic gradient. *Helgoland Mar Res* 51:433–443.
10. Linley EAS, Newell RC, Lucas MI (1983) Quantitative relationship between phytoplankton, bacteria and heterotrophic microflagellates in shelf waters. *Mar. Ecol. Prog Ser* 12:77-89.
11. Larsson U, Hagstrom A (1979) Phytoplankton exudate release as an energy source for the growth of pelagic bacteria. *Mar Bid* 52:199-206.
12. Lochte K, Bjernsen PK, Giesenhausen H, Weber A (1997) Bacterial standing stock and production and their relation to phytoplankton in the Southern Ocean. *Deep-Sea Res I* 44: 321-340.
13. Morel A, Prieur L (1977) Analysis of variations in ocean color. *Limnol. Oceanogr.* 22:709–722.
14. Moller Jensen (1983) Phytoplankton release of extracellular organic carbon molecular weight composition and bacterial assimilation. *Mar Ecol Prog Ser 11*: 39-48.
15. Nelson NB, Siegel DA (2002) Chromophoric DOM in the open ocean. In: Hansell D and Carlson C (eds.) Biogeochemistry of marine dissolved organic matter. Academic, San Diego, pp 547–578.
16. Porter K, Feig YS (1980) Enhanced detection of bacteria in natural environments by fluorochrome staining of DNA. *Limnol Oceanogr* 25: 948–951.
17. Parab S G, Matondkar S G P, Gomes H, Goes J I (2006) Monsoon driven changes in phytoplankton populations in the eastern Arabian Sea as revealed by microscopy and HPLC pigment analysis. *Cont Shelf Res* 26(20): 2538–2558.
18. Ramaiah N, Raghukumar S, Gauns M (1996) Bacterial abundance and production in the central and eastern Arabian Sea. *Curr Sci* 71 (11):878–882.

19. Sherr EB, Sherr BF (1993) Preservation and storage of samples for enumeration of heterotrophic protists. In Kemp P et al. (eds.) *Current Methods in Aquatic Microbial Ecology*. Lewis Publ, NY: 207–212.
20. Solanki HU, Mankodi PC, Nayak SR, Somvanshi VS (2005) Evaluation of remote-sensing-based potential fishing zones (PFZs) forecast methodology. *Cont Shelf Res* 25(8): 2163-2173.
21. Stewart FJ, Fritsen C.H (2004) Bacteria-algae relationships in Antarctic sea ice. *Antarctic Science* 16 (2): 143–156.
22. Strom SL (2000) Bacterivory: interactions between bacteria and their grazers. In Kirchman DL (ed.) *Microbial ecology of the oceans*. New York: Wiley-Liss, 351–386.
23. Wolter K (1982) Bacterial incorporation of organic substances released by natural phytoplankton populations. *Mar Ecol Prog Ser* 7:287-295.

Figures Captions

Fig.1 Cruise track of CRV *Sindhu Sankalp*- 009 during December 2010 showing sampling stations in the eastern Arabian Sea and Sardine fish-catch.

Fig.2 Distribution of Salinity during December 2010.

Fig.3 Surface distribution of microbial trophic components in relation to Chlorophyll *a* and CDOM along central west coast of India during December 2010: (a) Chl *a* ($\mu\text{g L}^{-1}$) (b) CDOM Ac300 (m^{-1}) (c) Total Bacterial Counts (cells L^{-1}) (d) HNF counts (cells L^{-1})

Fig.4 Match-up analysis of OCM-II derived Chl *a* with *insitu* Chl *a* (a) Correlation analysis and (b) Frequency distribution.

Fig.5 OCM-II images showing distribution of Chl *a* over the Eastern Arabian Sea during the Sardine-fishery season of December 2010. The study area is marked with red-box in the image panels

Fig. 6 Water-column distribution of microbial trophic components with respect to Chl *a* and CDOM.

Fig.7 Total bacteria and HNF distribution with respect to salinity.

Fig.8 Relationship between (a) Total bacteria and Chl *a* (b) HNF and Chl *a* (c) HNF and Chl *a*.

Fig.9 Overall relationships of CDOM with (a) Total bacterial counts and (b) Chl *a*.

Fig.10 Slope-ratio ($S_{275-295}:S_{350-450}$) characteristics of CDOM during the study period.

Fig.11 Relationship between : (a) Chl *a* and total phytoplankton density and (b) Surface Primary-productivity and Chl *a* off Dabhol-Shivardhan Sardine grounds.

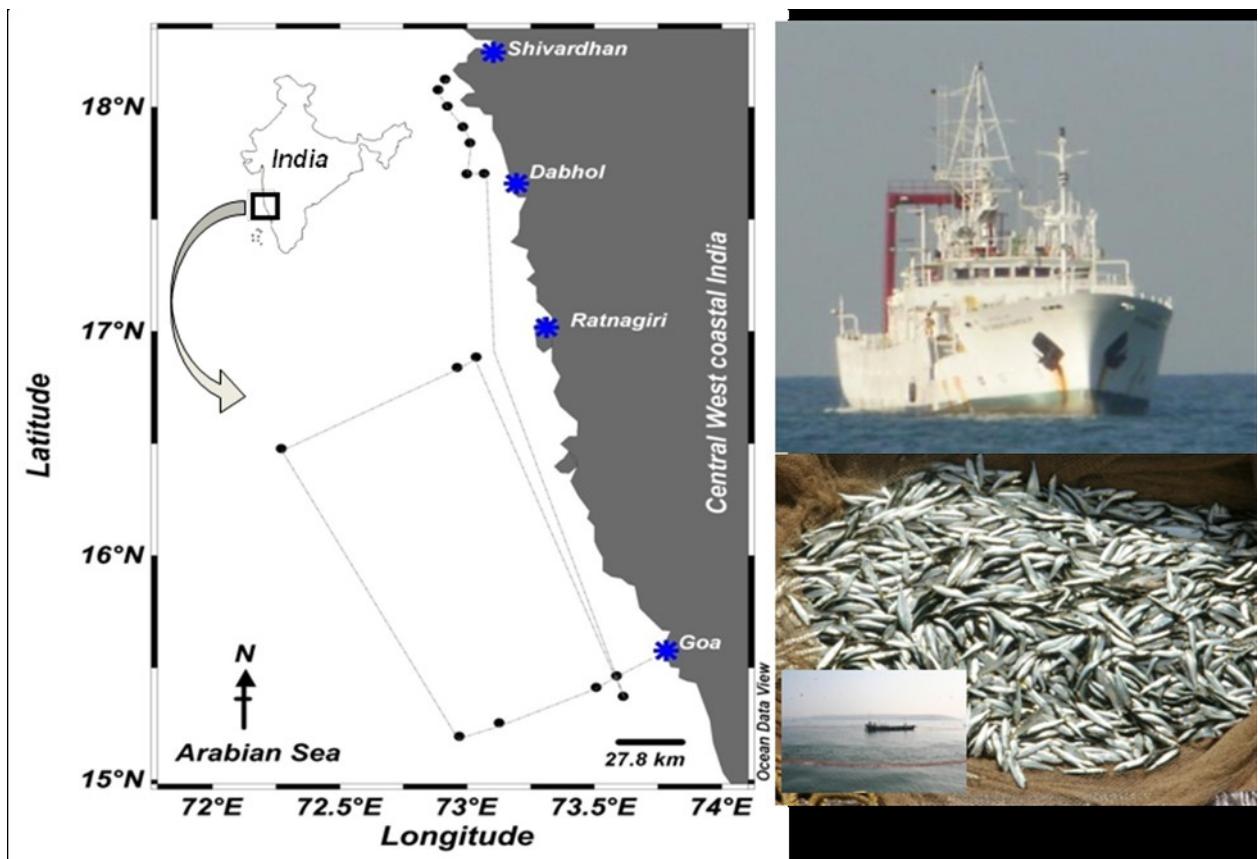


Fig.1 Cruise track of CRV *Sindhu Sankalp- 009* during December 2010 showing sampling stations in the eastern Arabian Sea and Sardine grounds.

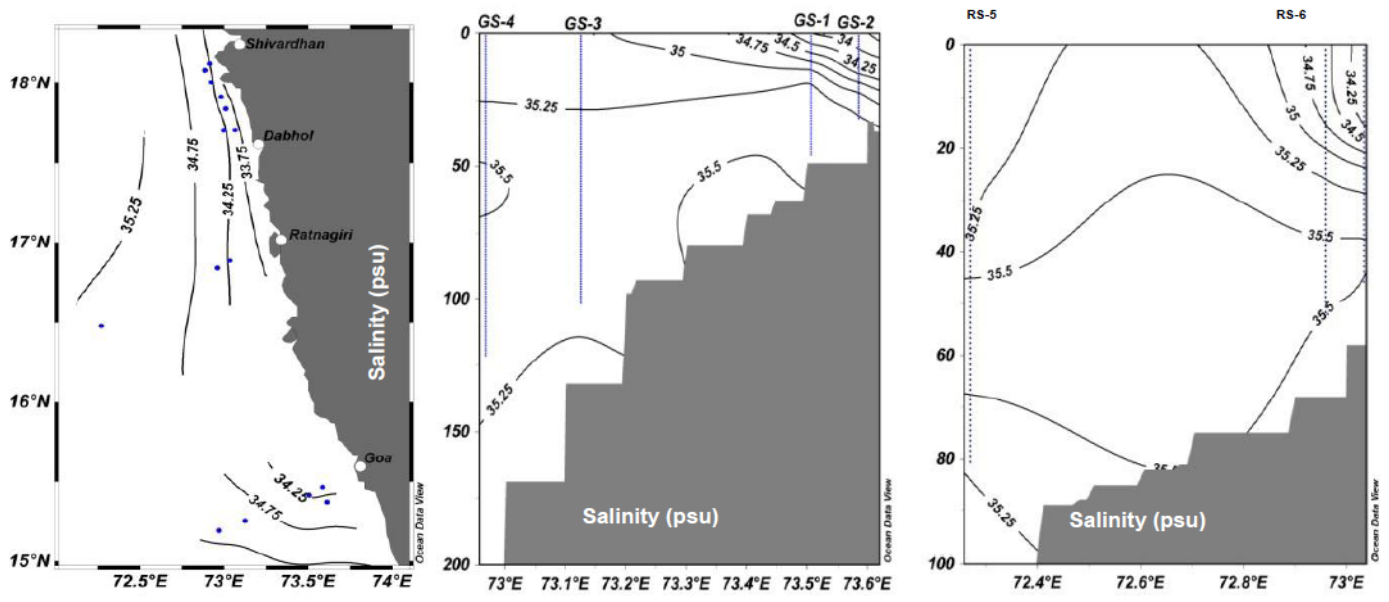


Fig.2 Distribution of Salinity during December 2010.

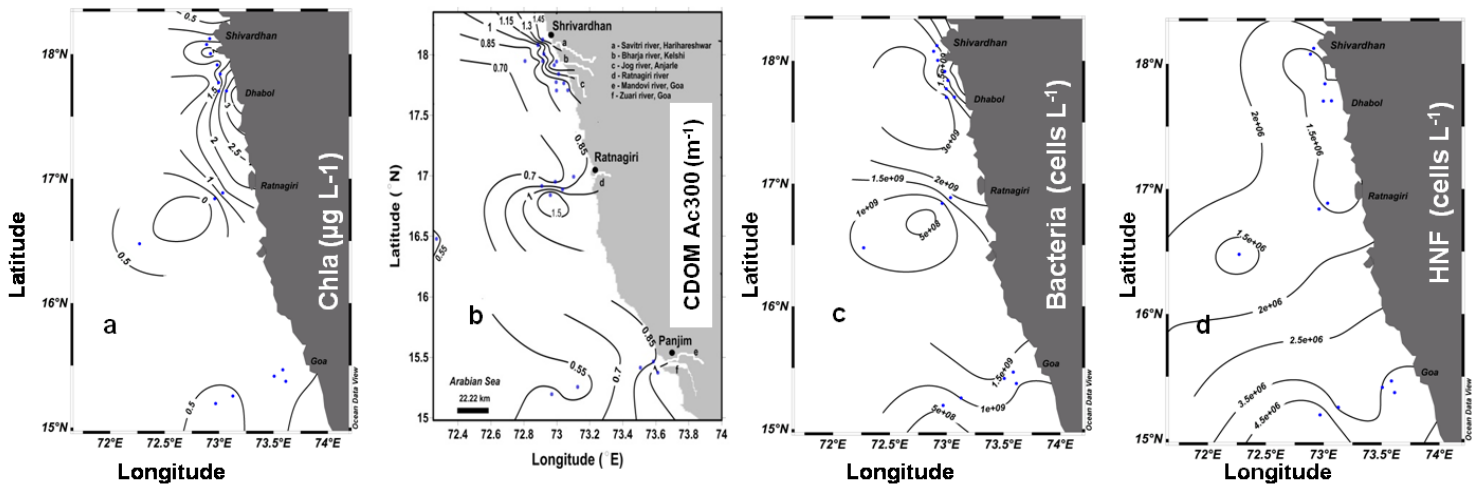


Fig.3 Surface distribution of microbial trophic components in relation to Chlorophyll *a* and CDOM along central west coast of India during December 2010: (a) Chl *a* ($\mu\text{g L}^{-1}$) (b) CDOM Ac300 (m^{-1}) (c) Total Bacterial Counts (cells L^{-1}) (d) HNF counts (cells L^{-1})

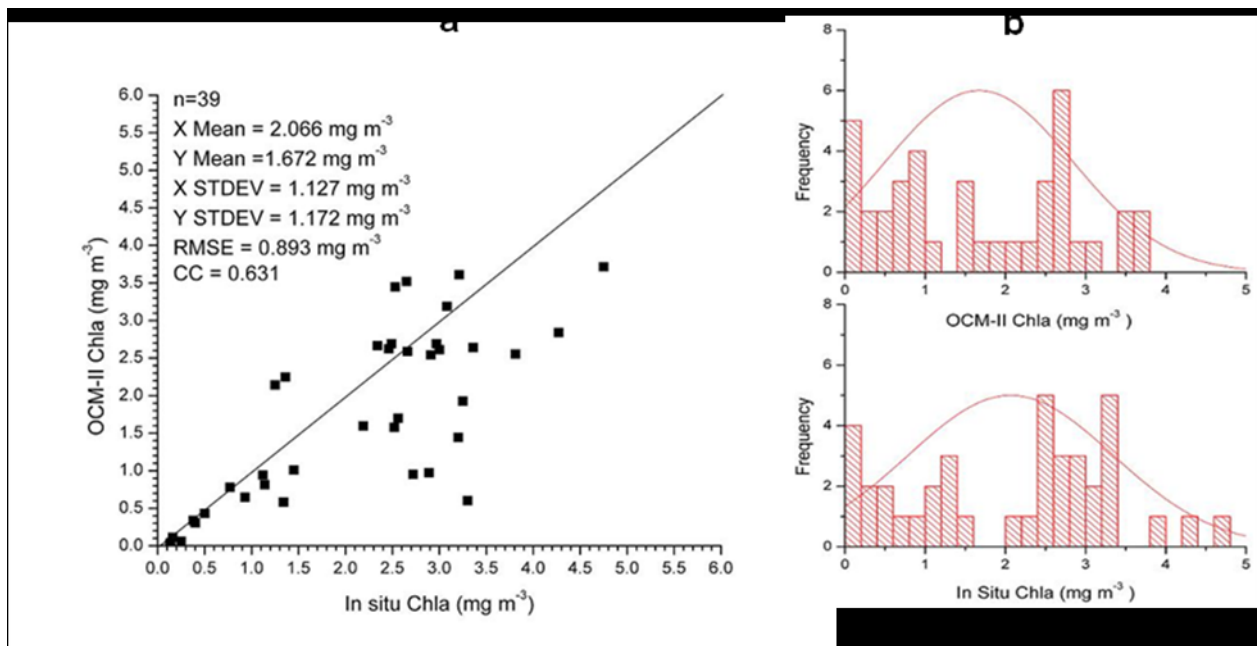


Fig.4 Match-up analysis of OCM-II derived Chl *a* with *insitu* Chl *a* (a) Correlation analysis and (b) Frequency distribution.

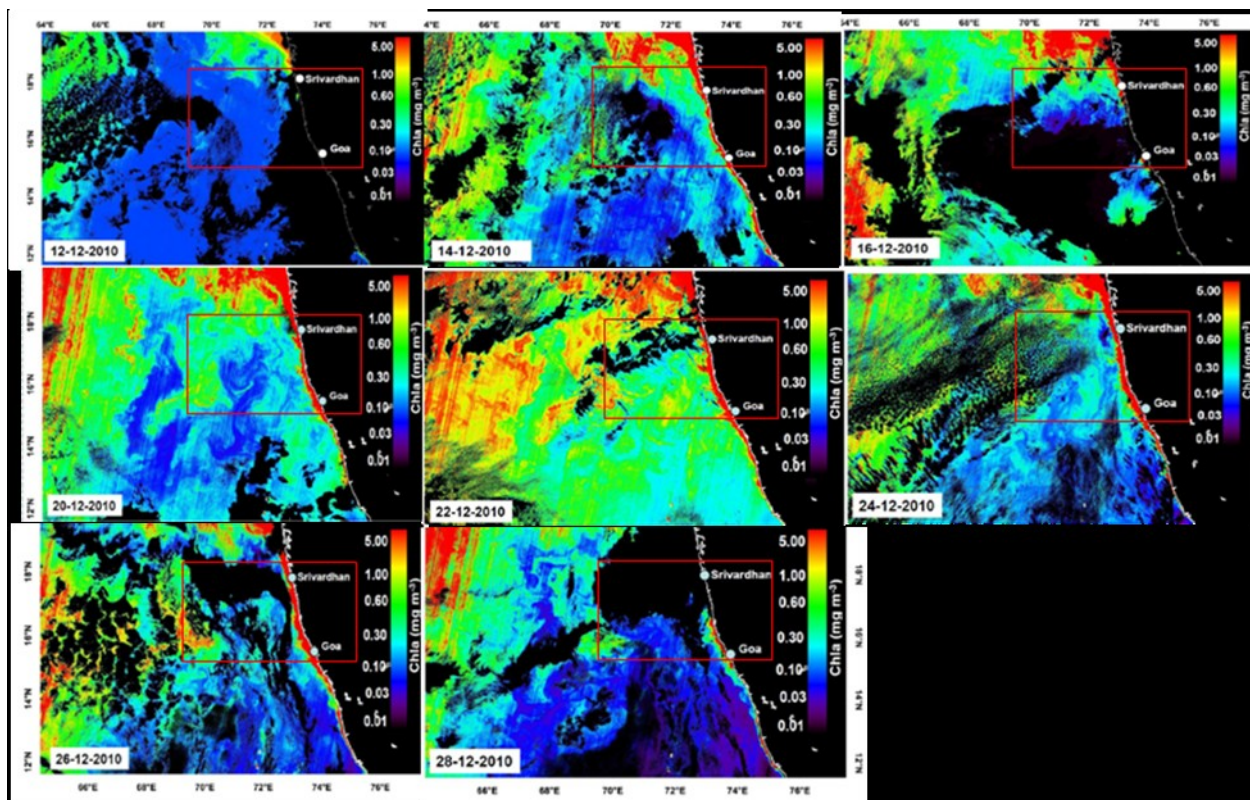


Fig 5 OCM-II images showing distribution of Chl *a* over the Eastern Arabian Sea during the Sardine-fishery season of December 2010. The study area is marked with red-box in the image panels.

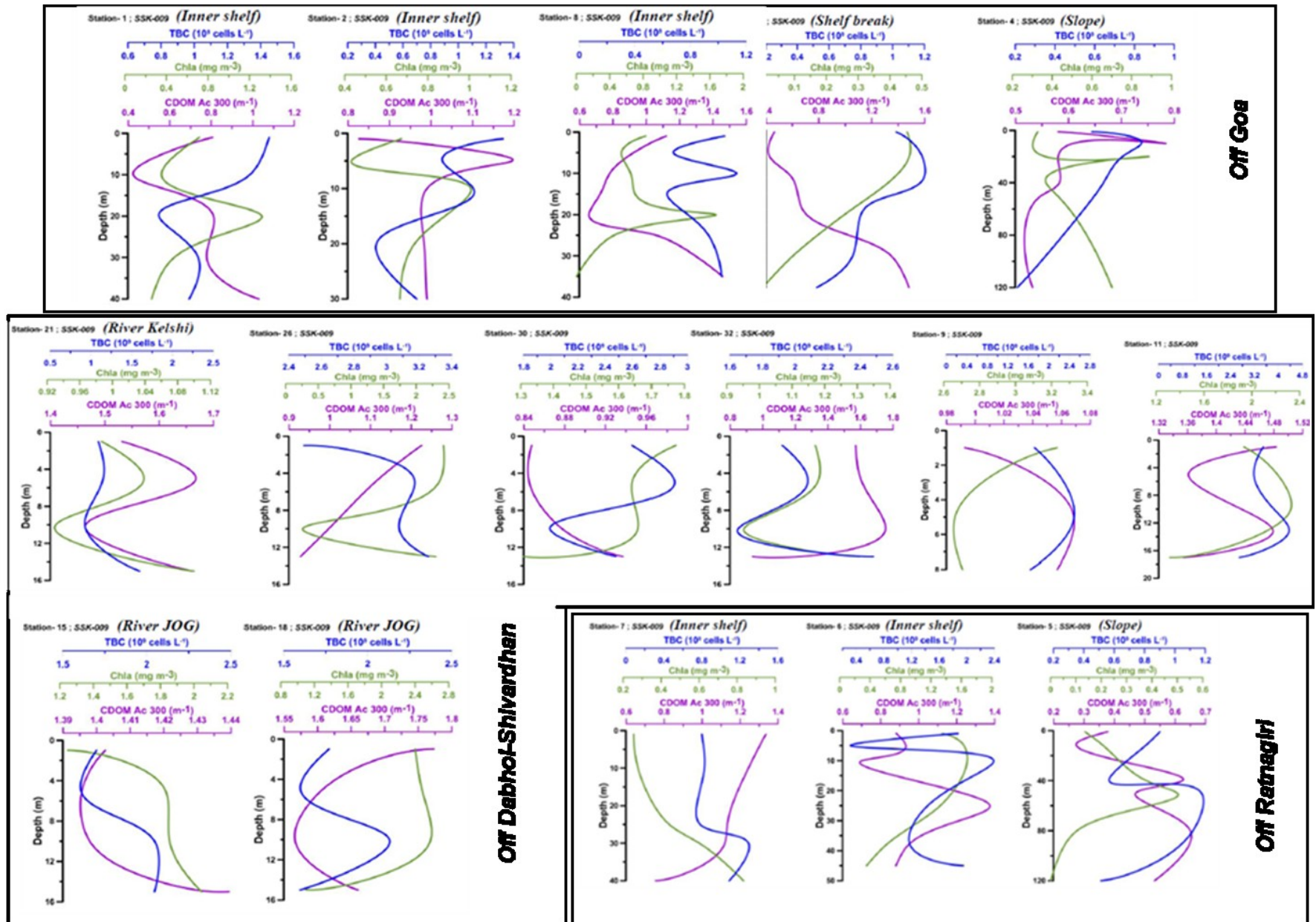


Fig. 6 Water-column distribution of microbial trophic components with respect to Chl *a*, CDOM.

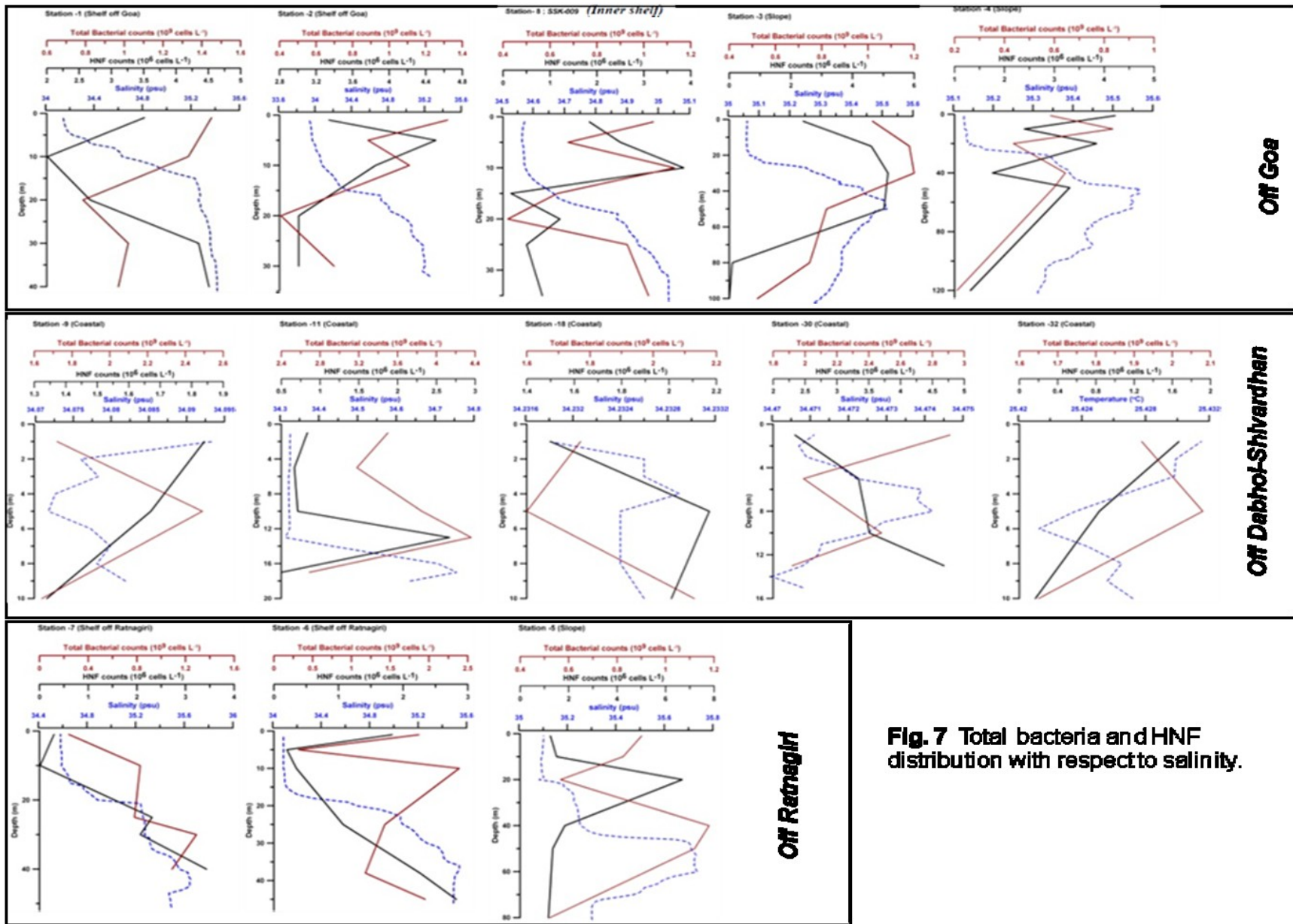


Fig. 7 Total bacteria and HNF distribution with respect to salinity.

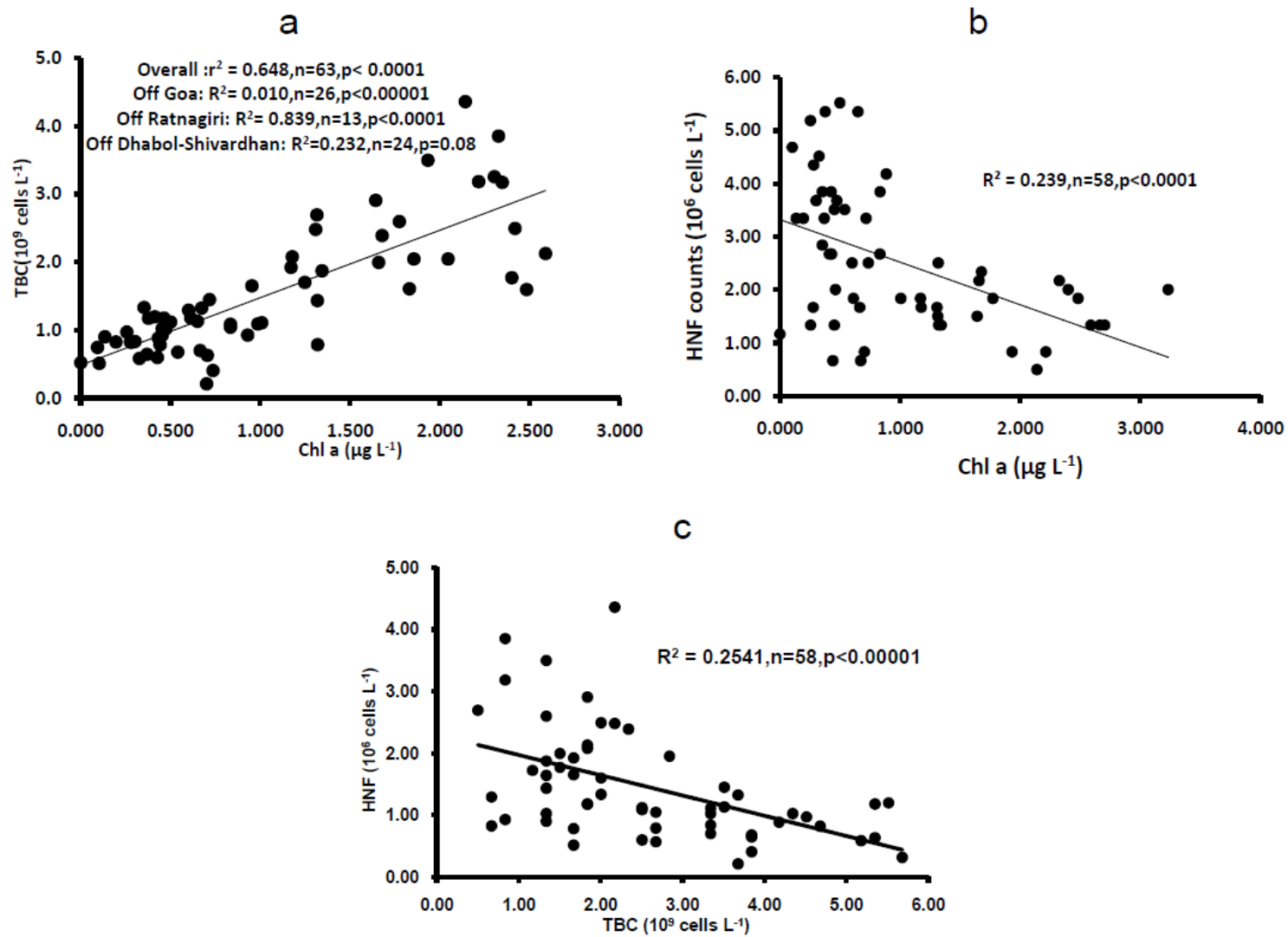


Fig.8 Relationship between (a) Total bacteria and Chl *a* (b) HNF and Chl *a* (c) HNF and Chl *a*

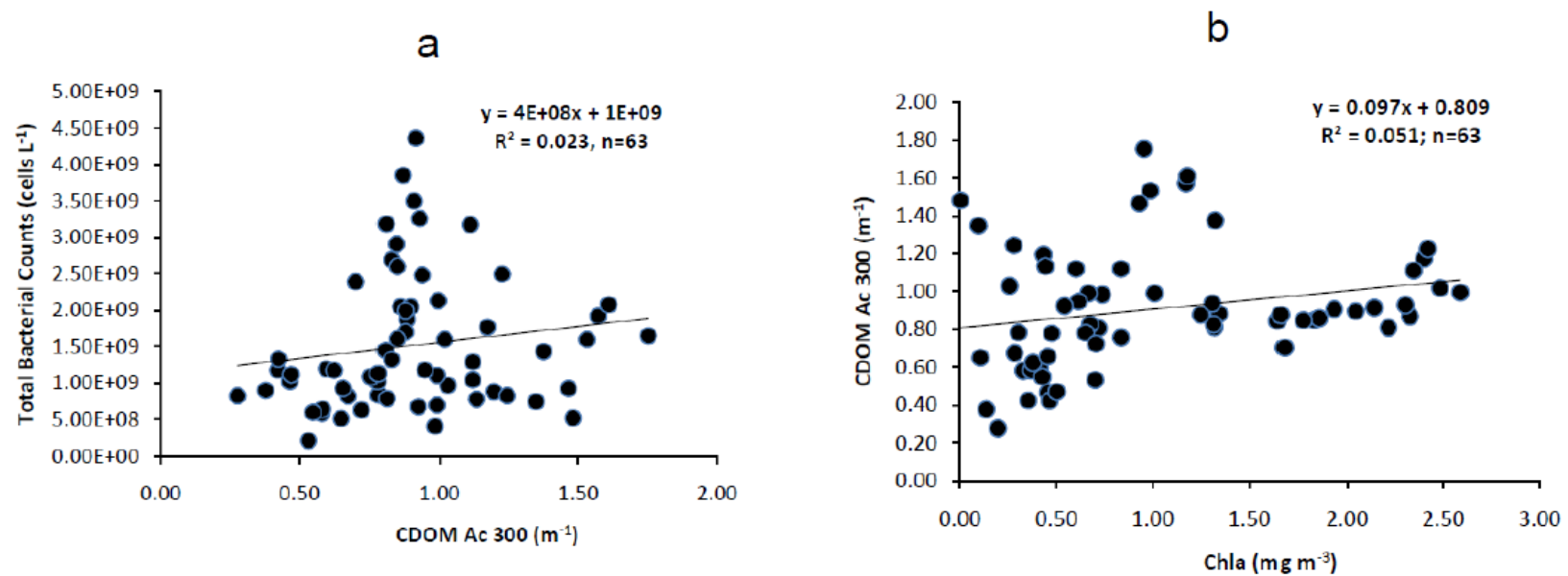


Fig.9 Overall relationships of CDOM with (a) Total bacterial counts and (b) Chl *a*

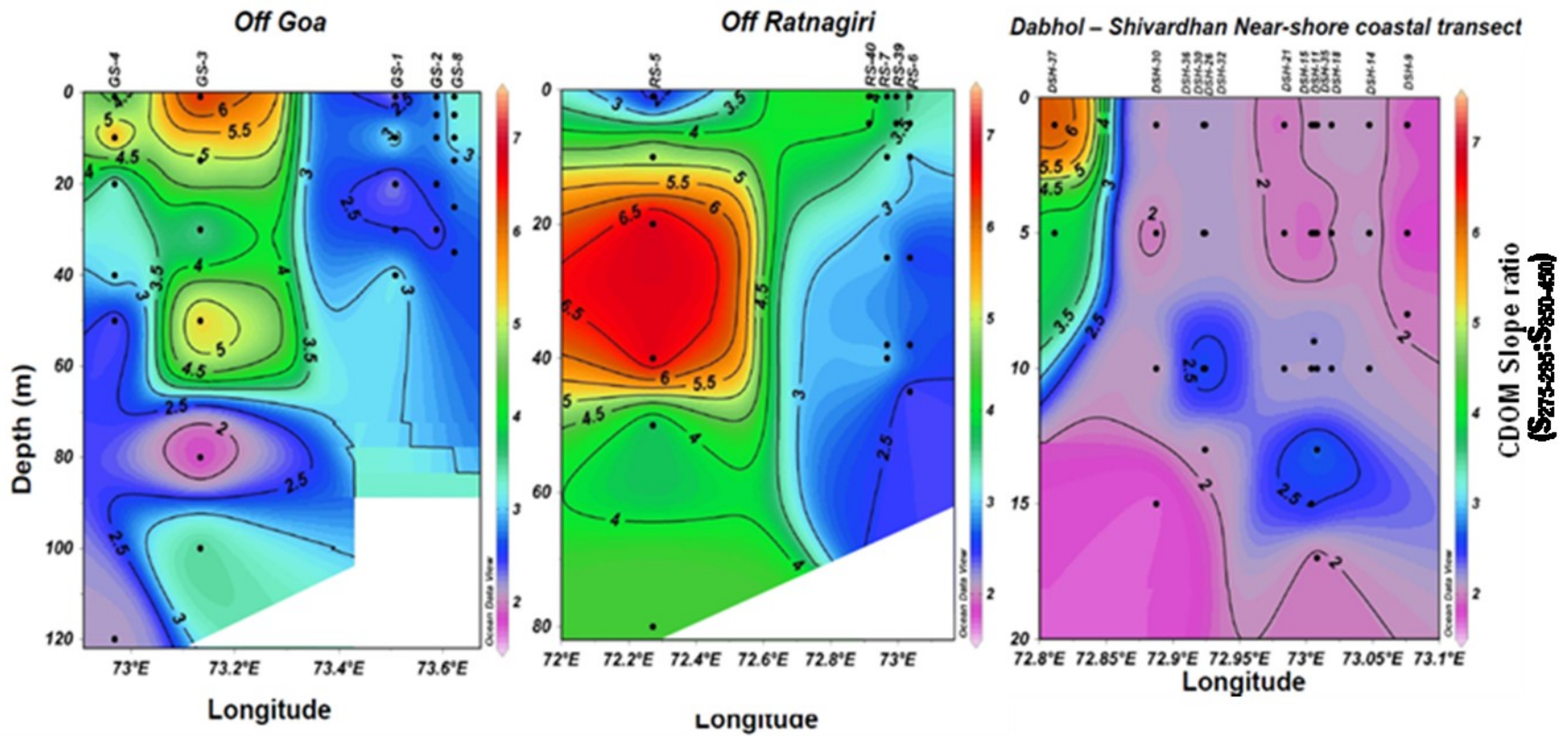


Fig.10 Slope-ratio ($S_{275-295}:S_{350-450}$) characteristics of CDOM during the study period.

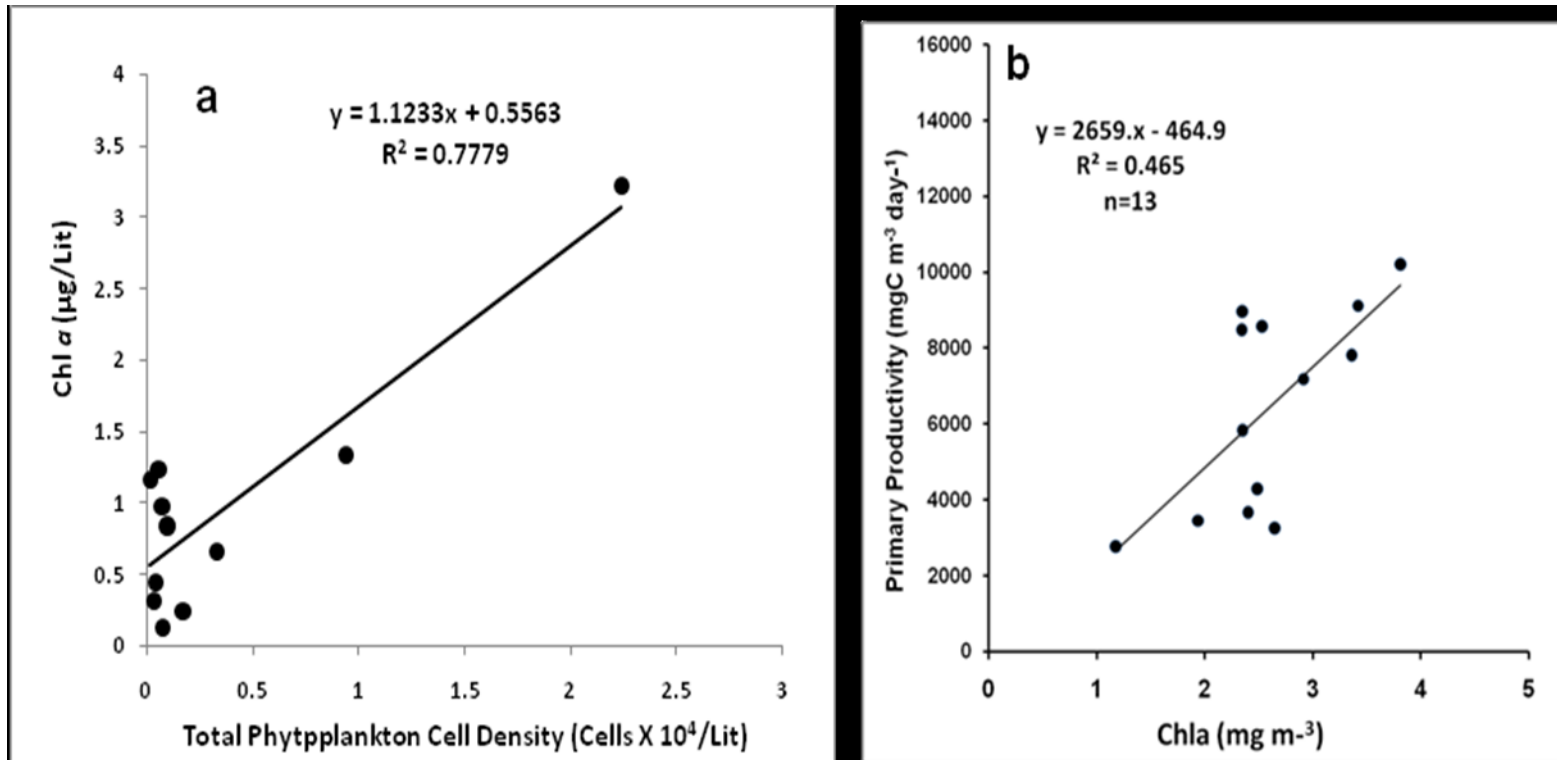


Fig.11 Relationship between : (a) |Chl *a* and total phytoplankton density and (b) Surface Primary-productivity and Chl *a* off Dabhol-Shivardhan Sardine fishing zone.